Inorg. Chem. **2002**, *41*, 239–248

New Monomeric Cobalt(II) and Zinc(II) Complexes of a Mixed N,S(alkylthiolate) Ligand: Model Complexes of (His)(His)(Cys) Metalloprotein Active Sites

SeChin Chang,[†] Vivek V. Karambelkar,[†] Roger D. Sommer,[‡] Arnold L. Rheingold,[‡] and David P. Goldberg*,[†]

Department of Chemistry, The Johns Hopkins University, Baltimore, Maryland 21218, and Department of Chemistry and Biochemistry, University of Delaware, Newark, Delaware 19716

Received March 23, 2001

The new N_2S(alkylthiolate) ligand 2-methyl-1-[methyl-(2-pyridin-2-ylethyl)amino]propane-2-thiolate, PATH (**1**), has been prepared and reacted with zinc(II) and cobalt(II) to give the monomeric complexes [(PATH)ZnBr] (**2**), [(PATH)-ZnNCS] (**3**), [(PATH)CoBr] (**4**), and [(PATH)CoNCS] (**5**). The molecular structures of **4** and **5** have been determined by X-ray diffraction. Each complex displays a distorted tetrahedral geometry at the metal center, with the PATH ligand providing the N_2S(alkylthiolate) donors. These complexes are close structural mimics of the active site of metalloproteins with a His_2Cys–M^{II} site such as that found in peptide deformylase. Complexes **4** and **5** are the first examples of crystallographically characterized Co^{II} complexes with an N_2SL (L ≠ N,S) donor set. Only one diastereomer for **2**–**5** is observed in the solid state, and simple molecular mechanics (Chem3D) calculations suggest this isomer is stable because of a favorable ligand conformation. NMR studies in the case of Zn^{II} and UV–vis studies in the case of Co^{II} provide strong evidence that their solid-state structures are retained in solution. Cyclic voltammetry reveals processes for both the $Co^{II/I}$ (**4**, − 1.51 V; **5**, − 1.49 V) and $Co^{III/II}$ (**4**, + 0.9 V; **5**, + 0.9 V) couples. The UV–vis data for the cobalt complexes are consistent with a monomeric, four-coordinate geometry regardless of the nature of the solvent (i.e., donating (MeOH, CH_3CN) vs nondonating (CH_2Cl_2)) and are compared with other cobalt complexes as well as cobalt-substituted His_2Cys metalloproteins (peptide deformylase and blue-copper proteins). In addition, reaction of the bromide complexes **2** and **4** with hydroxide anion leads to the formation of 1:1 hydroxide:M^{II} complexes which have been characterized in situ by ^1H NMR and UV–vis spectroscopy, respectively.

Introduction

Metalloproteins exert exquisite control over the reactivity of metal ions by judicious choice of donor ligands. In several cases, Nature has selected a mixed nitrogen/sulfur coordination environment for the metal cofactor, including blue copper proteins,[1] iron and cobalt nitrile hydratases,[2] cytidine deaminase,[3] bacteriophage T7 lysozyme,[4] spinach carbonic anhydrase,[5] alcohol dehydrogenase,[6,7] and peptide deformylase (PDF).[8] Of these diverse proteins, peptide deformylase is distinguished by certain interesting features. Although it has the conserved HEXXH motif characteristic of the well-known superfamily of zinc metallopeptidases (e.g., thermolysin),[9,10] PDF has recently been shown to contain an iron(II) ion in vivo.[11,12] Specifically, the iron center depicted

* Author to whom correspondence should be addressed. E-mail: dpg@jhu.edu.
[†] The Johns Hopkins University.
[‡] University of Delaware.

(1) (a) Randall, D. W.; Gamelin, D. R.; LaCroix, L. B.; Solomon, E. I. *J. Biol. Inorg. Chem.* **2000**, *5*, 16−29 and references therein. (b) Holm, R. H.; Kennepohl, P.; Solomon, E. I. *Chem. Rev.* **1996**, *96*, 2239−2314 and references therein.
(2) (a) Artaud, I.; Chatel, S.; Chauvin, A. S.; Bonnet, D.; Kopf, M. A.; Leduc, P. *Coord. Chem. Rev.* **1999**, *190*−*192*, 577−586. (b) Huang, W.; Jia, J.; Cummings, J.; Nelson, M.; Schneider, G.; Lindqvist, Y. *Structure* **1997**, *5*, 691−699.
(3) (a) Xiang, S.; Short, S. A.; Wolfenden, R.; Carter, C. W., Jr. *Biochemistry* **1996**, *35*, 1335−1341. (b) Betts, L.; Xiang, S.; Short, S. A.; Wolfenden, R.; Carter, C. W., Jr. *J. Mol. Biol.* **1994**, *235*, 635−656.
(4) Cheng, X.; Zhang, X.; Pflugrath, J. W.; Studier, F. W. *Proc. Natl. Acad. Sci. U.S.A.* **1994**, *91*, 4034−4038.
(5) (a) Rowlett, R. S.; Chance, M. R.; Wirt, M. D.; Sidelinger, D. E.; Royal, J. R.; Woodroffe, M.; Wang, Y.-F. A.; Saha, R. P.; Lam, M. G. *Biochemistry* **1994**, *33*, 13967−13976. (b) Bracey, M. H.; Christiansen, J.; Tovar, P.; Cramer, S. P.; Bartlett, S. G. *Biochemistry* **1994**, *33*, 13126−13131.
(6) Lipscomb, W. N.; Sträter, N. *Chem. Rev.* **1996**, *96*, 2375−2433.
(7) Vallee, B. L.; Auld, D. S. *Acc. Chem. Res.* **1993**, *26*, 543−551.

10.1021/ic010321r CCC: $22.00
Published on Web 12/21/2001

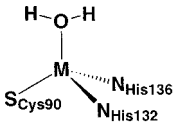

M = Fe^{II}, Zn^{II}, Co^{II}, Ni^{II}

Figure 1. The active site of peptide deformylase from *Escherichia coli*. The iron(II) form is found in vivo.

in Figure 1 is responsible for the hydrolytic cleavage of a formyl group at the N-terminus of newly formed polypeptides in bacterial cells. Thus PDF is the first example of a non-heme iron metallopeptidase, which is particularly intriguing since the inherent instability of Fe(II) toward oxidation implies that it is a poor choice for the catalysis of a non-redox-active reaction; this role is typically reserved for the inert Zn(II) ion. Interestingly, substitution of Fe(II)−PDF with cobalt(II) or nickel(II) results in active enzyme, but substitution with zinc(II) gives a relatively inactive protein toward formyl bond cleavage.[11] Given that these different metal-substituted forms of PDF contain essentially isostructural metal centers, it is important to delineate the factors responsible for the observed differences in reactivity. To this end, we are interested in synthesizing a family of N_2S(thiolate)−M^{II} compounds. Also, it is rare for a "zinc" metallopeptidase to have a cysteinate sulfur as the third ligand instead of an N or O donor from His or Glu/Asp.[6] A thiolate donor should have a large effect on the electronic properties of the metal center.

A postulated mechanism of formyl bond hydrolysis for PDF suggests that the function of the metal ion is to produce a nucleophilic hydroxide or water ligand in proximity to the substrate.[13,14] The pK_a and nucleophilicity of the catalytically active M−H_2O/OH moiety is significantly affected by the Lewis acidity of the M(II) ion, which in turn is likely dominated by the presence of a negatively charged cysteinate ligand.[15] Thus, model complexes that include an alkylthiolate ligand have particular relevance to peptide deformylase. Indeed, a general need for such model compounds has already been pointed out by workers attempting to characterize the active site of spinach carbonic anhydrase, which contains a $HisCys_2Zn^{II}$ active site.[5a]

Previously, synthetic efforts have been applied toward modeling the active site of N,S-containing metalloproteins, but inclusion of an alkylthiolate ligand has proven to be a particularly challenging synthetic goal.[16−21] Difficulties in handling alkylthiolate ligands include their facile oxidation to disulfide products[22] as well as their inherent propensity toward forming bridged, M−S(R)−M polynuclear species.[23] The only relatively easy syntheses are those of the neutral $[M^{II}N_2S_2]$ complexes (M = Zn, Co), of which there are several examples. However, the preparation of monomeric four-coordinate complexes of the type $[N_xS_yM^{II}L]$, where L is labile and *different from the N or S donor*, is a difficult synthetic problem and has prompted much effort in ligand design by our group[24] and others. Some recent successes include the synthesis of mixed N,S(alkylthiolate)−Cu(II) complexes as the first models for blue copper proteins,[25,26] and the preparation of monomeric $[N_2S$(alkylthiolate)ZnL] complexes by Carrano and co-workers.[27,28]

We have previously communicated the preparation of a new pyridine−amine−thiolate ligand, PATH (**1**), and its use in the synthesis of two new zinc(II) complexes that contain an N_2S(alkylthiolate)L donor set.[24] In this paper we describe the synthesis and structural characterization of the analogous cobalt(II) complexes, together wih a detailed description of the synthesis, solution, and solid-state structures and stereochemical preferences of both the Zn^{II} and Co^{II} complexes. In addition, evidence is provided for the formation of [(PATH)Zn(OH)] and [(PATH)Co(OH)] complexes.

The Co^{II} ion has been used as an important spectroscopic probe for PDF[13] as well as many other proteins that have an N,S(thiolate)-ligated metal center, such as the ubiquitous zinc

(8) For crystal structures of PDF, see the following. (a) Hao, B.; Gong, W.; Rajagopalan, P. T. R.; Zhou, Y.; Pei, D.; Chan, M. K. *Biochemistry* **1999**, *38*, 4712−4719. (b) Becker, A.; Schlichting, I.; Kabsch, W.; Schultz, S.; Wagner, A. F. V. *J. Biol. Chem.* **1998**, *273*, 11413−11416. (c) Becker, A.; Schlichting, I.; Kabsch, W.; Groche, D.; Schultz, S.; Wagner, A. F. V. *Nat. Struct. Biol.* **1998**, *5*, 1053−1058. (d) Chan, M. K.; Gong, W.; Rajagopalan, P. T. R.; Hao, B.; Tsai, C. M.; Pei, D. *Biochemistry* **1997**, *36*, 13904−13909.
(9) Vallee, B. L.; Auld, D. S. *Biochemistry* **1990**, *29*, 5647−5659.
(10) Holmes, M. A.; Matthews, B. W. *J. Mol. Biol.* **1982**, *160*, 623−629.
(11) Groche, D.; Becker, A.; Schlichting, I.; Kabsch, W.; Schultz, S.; Wagner, A. F. V. *Biochem. Biophys. Res. Commun.* **1998**, *246*, 342−346.
(12) Rajagopalan, P. T. R.; Yu, X. C.; Pei, D. *J. Am. Chem. Soc.* **1997**, *119*, 12418−12419.
(13) Rajagopalan, P. T. R.; Grimme, S.; Pei, D. *Biochemistry* **2000**, *39*, 779−790.
(14) Chin, J. *Acc. Chem. Res.* **1991**, *24*, 145−152.
(15) For work describing the effect of Cys ligation on the metal center in mutant forms of carbonic anhydrase, see the following. (a) Christianson, D. W.; Fierke, C. A. *Acc. Chem. Res.* **1996**, *29*, 331−339. (b) Kiefer, L. L.; Fierke, C. A. *Biochemistry* **1994**, *33*, 15233−15240.
(16) Brand, U.; Vahrenkamp, H. *Inorg. Chim. Acta* **2000**, *308*, 97−102 and references therein.
(17) Parkin, G. *Chem. Commun.* **2000**, 1971−1985.
(18) Grapperhaus, C. A.; Tuntulani, T.; Reibenspies, J. H.; Darensbourg, M. Y. *Inorg. Chem.* **1998**, *37*, 4052−4058.
(19) Grapperhaus, C. A.; Darensbourg, M. Y. *Acc. Chem. Res.* **1998**, *31*, 451−459.
(20) Kaptein, B.; Barf, G.; Kellogg, R. M.; Bolhuis, F. V. *J. Org. Chem.* **1990**, *55*, 1890−1901.
(21) For recent work on mixed N,S model complexes in which the S is not an alkylthiolate, see the following. (a) Kimblin, C.; Bridgewater, B. M.; Hascall, T.; Parkin, G. *J. Chem. Soc., Dalton Trans.* **2000**, 1267−1274. (b) Kimblin, C.; Bridgewater, B. M.; Churchill, D. G.; Hascall, T.; Parkin, G. *Inorg. Chem.* **2000**, *39*, 4240−4243. (c) Chiou, S.-J.; Innocent, J.; Riordan, C. G.; Lam, K.-C.; Liable-Sands, L.; Rheingold, A. L. *Inorg. Chem.* **2000**, *39*, 4347−4353. (d) Berreau, L. M.; Makowska-Grzyska, M. M.; Arif, A. M. *Inorg. Chem.* **2000**, *39*, 4390−4391. (e) Berreau, L. M.; Allred, R. A.; Makowska-Grzyska, M. M.; Arif, A. M. *Chem. Commun.* **2000**, 1423−1424. (f) Chiou, S.-J.; Ge, P.; Riordan, C. G.; Liable-Sands, L. M.; Rheingold, A. L. *Chem. Commun.* **1999**, 159−160. (g) Ghosh, P.; Parkin, G. *Chem. Commun.* **1998**, 413−414. (h) Kimblin, C.; Hascall, T.; Parkin, G. *Inorg. Chem.* **1997**, *36*, 5680−5681.
(22) For recent examples, see the following. (a) Ohta, T.; Tachiyama, T.; Yoshizawa, K.; Yamabe, T.; Uchida, T.; Kitagawa, T. *Inorg. Chem.* **2000**, *39*, 4358−4369. (b) Ohta, T.; Tachiyama, T.; Yoshizawa, K.; Yamabe, T. *Tetrahedron Lett.* **2000**, *41*, 2581−2585.
(23) Müller, B.; Schneider, A.; Tesmer, M.; Vahrenkamp, H. *Inorg. Chem.* **1999**, *38*, 1900−1907 and references therein.
(24) Chang, S.; Karambelkar, V. V.; diTargiani, R. C.; Goldberg, D. P. *Inorg. Chem.* **2001**, *40*, 194−195.
(25) Holland, P. L.; Tolman, W. B. *J. Am. Chem. Soc.* **2000**, *122*, 6331−6332.
(26) Holland, P. L.; Tolman, W. B. *J. Am. Chem. Soc.* **1999**, *121*, 7270.
(27) Hammes, B. S.; Carrano, C. J. *J. Chem. Soc., Dalton Trans.* **2000**, 3304−3309.
(28) Hammes, B. S.; Carrano, C. J. *Chem. Commun.* **2000**, 1635−1636.

finger and blue copper proteins. In light of of this work, spectroscopic characterization of N,S(alkylthiolate) cobalt(II) model compounds is of particular interest. To our knowledge, [(PATH)CoBr] and [(PATH)CoNCS] are the first crystallographically characterized cobalt(II) complexes with an N_2SL coordination environment. Thus the spectroscopic features of our PATH−cobalt model complexes, including UV−vis and electrochemical data, are described in detail. In addition, NMR and UV−vis evidence shows that the displacement of the Br^- ligand in **2** and **4** by OH^- anion proceeds smoothly to form hydroxide complexes in situ.

Experimental Section

Materials and General Methods. For the cobalt complexes, all preparations were carried out under an argon atmosphere using standard Schlenk techniques. The protonated form of the ligand, PATH−H, and the zinc complexes were prepared in the air. Isobutylene oxide (TCI), 2-(2-methylaminoethyl)pyridine (Aldrich), reagent grade solvents, and all other commercially available reagents were used as received. Isobutylene sulfide was prepared according to a known procedure.[29] Column chromatography was performed with Natland International Corp. silica gel 60, 200−400 mesh. ^{1}H and ^{13}C NMR spectra were recorded on a Varian Unity plus 400 spectrometer (400 MHz) at ambient probe temperature with tetramethylsilane as the internal reference. Electronic absorption spectra were taken on a HP 8453 UV−visible spectrophotometer. Infrared spectra were measured using a 4030 Galaxy series FT-IR spectrometer. Mass spectra were recorded at the Mass Spectrometry Laboratory, Department of Chemistry, Johns Hopkins University, using a VG analytical 70-S mass spectrometer. Melting points were measured with a Thomas-Hoover apparatus. Elemental analyses were recorded at the Atlantic Microlab, Inc., Norcross, GA.

2-Methyl-1-[methyl(2-pyridin-2-ylethyl)amino]propane-2-thiol (PATH−H). A solution of isobutylene sulfide (7.12 g, 80.8 mmol) in CH_3CN (80 mL) was added dropwise to a solution of 2-(2-methylaminoethyl)pyridine (10.0 g, 73.4 mmol) in CH_3CN (40 mL) over 1 h. The mixture was refluxed for 16 h, and the solvent was evaporated. The resulting yellow-orange oil was purified by flash chromatography on silica gel (CH_2Cl_2:MeOH, 19:1) to give PATH−H as a light yellow oil (8.50 g, 52%).^{1}H NMR (400 MHz, $CDCl_3$): δ 1.25 (s, 6H, CH_3), 2.07 (s, br, SH), 2.46 (s, 3H, N−CH_3), 2.48 (s, 2H, CH_2), 2.93−2.95 (m, 4H, CH_2CH_2), 7.10 (ddd, $J_{\beta-\gamma}$ = 7.6 Hz, $J_{\beta-\alpha}$ = 4.9 Hz, $J_{\beta-\delta}$ = 1.1 Hz, 1H, H_β), 7.18 (d, $J_{\delta-\gamma}$ = 7.8 Hz, 1H, H_δ), 7.58 (ddd, $J_{\gamma-\beta}$ = 7.6 Hz, $J_{\gamma-\delta}$ = 7.6 Hz, $J_{\gamma-\alpha}$ = 1.8 Hz, 1H, H_γ), 8.52 (m, 1H, H_α). ^{13}C NMR (100 MHz, $CDCl_3$): δ 30.2, 36.5, 44.7, 46.4, 60.4, 71.6, 121.1, 123.4, 136.2, 149.3, 160.6. MS(FAB): *m*/*z* 225.0 ([M + H]$^+$, calcd 224.1)

[(PATH)ZnBr] (2). The sodium thiolate of PATH−H was generated by addition of NaOH (0.020 g, 0.51 mmol) to PATH−H (0.104 g, 0.46 mmol) in MeOH (10 mL). Once the NaOH was consumed, the solution was added dropwise to $ZnBr_2$ (0.104 g, 0.46 mmol) in MeOH (5 mL). The reaction mixture was stirred for 4 h and then filtered to give a white powder, which was washed with a small amount of cold Et_2O and dried under vacuum to give 0.125 g (73%) of **2**. Colorless crystals of **2** were obtained from MeOH/Et_2O for the X-ray diffraction study. Mp: 224−227 °C. ^{1}H NMR (400 MHz, $CDCl_3$): δ 1.39 (s, 3H, CH_3), 1.61 (s, 3H, CH_3), 2.58 (d, J = 13.0, 1H, CH_2), 2.80 (s, 3H, N−CH_3), 2.82−3.09 (m, 4H, CH_2CH_2), 3.58 (m, 1H, CH_2), 7.34 (d, $J_{\delta-\gamma}$ = 7.8 Hz, 1H, H_δ), 7.47 (m, 1H, H_β), 7.89 (ddd, $J_{\gamma-\delta}$ = 7.8 Hz, $J_{\gamma-\beta}$ = 7.8 Hz, $J_{\gamma-\alpha}$ = 1.7 Hz, 1H, H_γ), 8.84 (m, 1H, H_α). ^{13}C NMR (100 MHz, $CDCl_3$): δ 32.3, 33.8, 35.3, 46.0, 49.8, 59.9, 73.6, 126.6, 125.0, 140.3, 149.8, 159.5 Anal. Found: C, 38.46; H, 5.23; N, 7.39. Calcd for $C_{12}H_{19}N_2SZnBr$: C, 39.35; H, 5.23; N, 7.65. MS(FAB): *m*/*z* 367.1 ([M + H]$^+$, calcd 366.0)

[(PATH)ZnNCS] (3). To a solution of PATH−H (0.282 g, 1.25 mmol) in MeOH (10 mL) was added NaOH (0.055 g, 1.38 mmol) in MeOH (5 mL). The resulting mixture was stirred under argon for 0.5 h at room temperature. A solution of $ZnBr_2$ (0.282 g, 1.25 mmol) in MeOH (5 mL) was added to the above solution and allowed to stir for 5 min, at which point KSCN (0.731 g, 7.52 mmol) was added in methanol (5 mL). The reaction mixture was stirred for 15 min, during which time a fine white precipitate formed. MeOH (50 mL) was added, and the reaction mixture was heated to 55 °C until a clear solution was obtained. The volume was reduced to 15 mL and allowed to stand for 18 h to give 0.296 g of pure **3** (68%) as a crystalline solid. Mp: 214−217 °C. ^{1}H NMR (400 MHz, CD_3CN): δ 1.29 (s, 3H, CH_3), 1.46 (s, 3H, CH_3), 2.53 (d, 1H, CH_2), 2.67 (s, 3H, N−CH_3), 2.75−2.90 (m, 2H, CH_2), 3.00−3.10 (m, 2H, CH_2), 3.27−3.33 (m, 1H, CH_2), 7.49 (d, $J_{\delta-\gamma}$ = 8 Hz, 1H, H_δ), 7.56 (t, $J_{\beta-\gamma}$ = 6 Hz, 1H, H_β), 8.01 (ddd, $J_{\gamma-\beta}$ = 8 Hz, 1H, H_γ), 8.54 (d, $J_{\alpha-\beta}$ = 5 Hz, 1H, H_α). ^{13}C NMR (100 MHz, CD_3CN): δ 33.0, 34.3, 36.0, 46.7, 49.8, 60.5, 74.1, 124.8, 126.9, 142.2, 149.8, 161.9 (*SCN* not found). IR (CH_2Cl_2): 2065 cm^{-1} (SCN stretch). Anal. Calcd for $C_{13}H_{19}N_3S_2Zn$: C, 45.33; H, 5.49; N, 12.04. Found: C, 45.06; H, 5.61; N, 12.05. MS(FAB): *m*/*z* 345.1 ([M]$^+$, calcd 345.03).

[(PATH)CoBr] (4). The sodium thiolate of PATH−H was generated by the addition of NaOH (0.085 g, 2.10 mmol) to a solution of PATH−H (0.43 g, 1.92 mmol) in MeOH (8 mL). Once the NaOH was consumed, the solution was added dropwise to a solution of $CoBr_2$ (0.42 g, 1.92 mmol) in MeOH (15 mL). The solution was stirred for 10 h and then filtered to isolate the product as a blue-purple powder, which was washed with a small amount of cold methanol and dried under vacuum. The yield of **4** was 0.49 g (71%). For X-ray diffraction studies, cobalt-blue crystals of **4** were obtained by vapor diffusion methods in CH_2Cl_2/diethyl ether. Mp: 226−228 °C. UV−vis (CH_3CN): λ_{max}, nm (ϵ, M^{-1} cm^{-1}) 315 (3032), 388 (1294), 414 (1465), 538 (270), 643 (sh, 460), 672 (522). Anal. Found: C, 39.97; H, 5.73; N, 7.11. Calcd for $C_{12}H_{19}N_2SCoBr$: C, 39.77; H, 5.29; N, 7.74. MS(FAB): *m*/*z* 362.0 ([M + H$^+$], calcd 361.0).

[(PATH)CoNCS] (5). The sodium thiolate of PATH−H was generated by the addition of NaOH (0.059 g, 1.34 mmol) to a solution of the PATH−H ligand (0.30 g, 1.34 mmol) in MeOH (10 mL). Once the NaOH was consumed, the solution was added dropwise to a solution of $Co(NCS)_2$ (0.23 g, 1.34 mmol) in MeOH (10 mL). The solution was stirred for 12 h and then filtered to give **5** as a hunter-green powder, which was washed with a small amount of cold methanol and dried under vacuum. The yield of **5** was 0.27 g (59%). Dark green crystals of **5** were obtained by vapor diffusion methods in CH_2Cl_2/diethyl ether for X-ray diffraction studies. UV−vis (CH_3CN): λ_{max}, nm (ϵ, M^{-1} cm^{-1}) 326 (3861), 375 (1332), 443 (877), 517 (290), 622 (394), 669 (489). IR (CH_2Cl_2): 2077 cm^{-1} (SCN stretch). Anal. Found: C, 44.97; H, 5.54; N, 11.99. Calcd for $C_{13}H_{19}N_3S_2Co$: C, 45.88; H, 5.63; N, 12.35.

Formation of [(PATH)M^{II}(OH)] (M = Zn, Co). The formation of [(PATH)Zn(OH)] in situ was monitored by ^{1}H NMR spectroscopy. To a solution of [(PATH)ZnBr] in CD_3OD (1.0 mL, 13.6 × 10^{-3} M) were added successive amounts (10 μL, 0.2 equiv) of a stock solution (0.271 M) of NaOH in D_2O. The reaction mixture was stirred for 5 min after each addition of OH^-, an aliquot (0.5

(29) Darensbourg, M. Y. *Inorganic Syntheses*; John Wiley & Sons: 1998; Vol. 32, pp 94−96.

Scheme 1

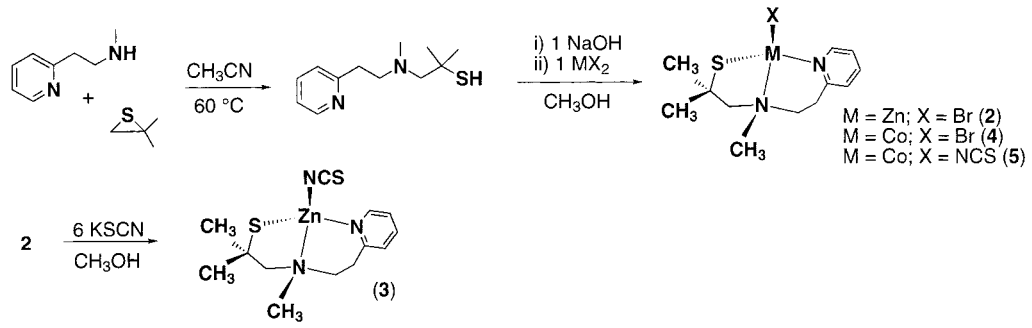

mL) was then transferred to an NMR tube, and the ^{1}H NMR spectrum was recorded at 24 °C. The aliquot was then recombined with the reaction mixture. A total of 70 μL of NaOH solution was added, equal to 1.4 equiv of zinc complex.

The formation of [(PATH)CoOH] was monitored by UV−vis spectroscopy. A solution of [(PATH)CoBr] in MeOH (50 mL, 2.54 $\times$ 10^{-3} M) was prepared in a three-neck flask attached via a U-tube to a 1.0 cm path length cuvette under an Ar atmosphere. A concentrated stock solution of NaOH in H_2O (0.128 M) was added in successive amounts (100 μL) by gastight syringe to the [(PATH)-CoBr] solution. The solution was stirred for 10 min after each addition, and then the apparatus was tilted to fill the cuvette and the absorption spectrum was recorded.

Electrochemistry. Cyclic voltammograms were measured with a BAS-23 potentiostat. A three-electrode configuration made up of a glassy carbon working electrode, a Ag/AgCl reference electrode (3 M NaCl), and a platinum wire auxiliary electrode was employed. Measurements were performed at ambient temperature under nitrogen with 0.2 M tetra-*n*-butylammonium hexafluorophosphate as the supporting electrolyte. Potentials are reported vs Ag/AgCl in 3 M NaCl. The ferrocenium/ferrocene (Cp_2Fe^{III}/Cp_2Fe^{II}) couple was observed at 0.455 V under these conditions.

Crystal Structure Determination. Suitable crystals were selected and mounted on thin glass fibers using epoxy. Diffraction data were collected using a Siemens P4 diffractometer equipped with a CCD detector. Preliminary unit-cell determinations were obtained by harvesting reflections from three orthogonal sets of 15 frames, using −0.3° ω scans. These results were confirmed by refinement of unit-cell parameters during integration. Crystallographic information is summarized in Table 1. All structures were solved using direct methods. Non-hydrogen atoms were located by difference Fourier synthesis and were refined anisotropically. Hydrogen atoms were added at calculated positions and treated as isotropic contributions with thermal parameters defined as 1.2 or 1.5 times that of the parent atom. All software and sources of scattering factors are contained in the SHELXTL program library (version 5.10, G. Sheldrick, Bruker-AXS, Madison, WI).

Results and Discussion

Synthesis of PATH−H. The synthesis of 2-methyl-1-[methyl(2-pyridin-2-ylethyl)amino]propane-2-thiol (PATH−H) was accomplished in one step from commercially available precursors as shown in Scheme 1. On a large scale (>40 g) it proved economical to prepare the isobutylene sulfide from the epoxide following known procedures.[29] Ring opening of the sulfide to give the desired product proceeded smoothly in refluxing CH_3CN, and purification by silica gel chromatography was straightforward. There was no evidence of disulfide after purification, and the ligand can be stored as a solution in CH_2Cl_2 in a freezer (−20 °C) for at least 2 months without any decomposition as monitored by ^{1}H NMR spectroscopy.

Table 1. Crystallographic Data and Structure Refinement Parameters for [(PATH)CoBr] (**4**) and [(PATH)CoNCS] (**5**)

	[(PATH)CoBr]	[(PATH)CoNCS]
formula	$C_{12}H_{19}BrCoN_2S$	$C_{13}H_{19}CoN_3S_2$
fw	362.19	340.36
space group	$P2_1/n$	$P2_1/n$
a, Å	8.1867(7)	7.8132(18)
b, Å	14.9939(13)	14.733(3)
c, Å	11.9478(10)	14.012(4)
α, deg		
β, deg	91.096(2)	102.072(6)
γ, deg		
V, Å3	1466.3(2)	1577.3(6)
Z, *Z*′	4, 1	4, 1
cryst color, habit	blue parallelepiped	green needle
D(calcd), g cm^{-3}	1.641	1.433
μ(Mo Kα), cm^{-1}	40.18	13.43
temp, K	173(2)	173(2)
diffractometer	Siemens P4/CCD	
radiation	Mo Kα (λ = 0.71073 Å)	
$R(F)$, %[a]	5.16	3.30
$R(wF^2)$, %[a]	13.52	7.43

[a] Quantity minimized = $R(wF^2) = \sum[w(F_o^2 - F_c^2)^2]/\sum[(wF_o^2)^2]^{1/2}$; $R = \sum\Delta/\sum(F_o)$, $\Delta = |(F_o - F_c)|$, $w = 1/[\sigma^2(F_o^2) + (aP)^2 + bP]$, $P = [2F_c^2 + \mathrm{Max}(F_o,0)]/3$.

Synthesis of Zn^{II} and Co^{II} Complexes. Synthesis of [(PATH)ZnBr] (**2**) was carried out by addition of PATH in MeOH to a solution of $ZnBr_2$. The [(PATH)ZnNCS] (**3**) complex was prepared by formation of the bromide complex in situ, followed by addition of excess KSCN. Both complexes precipitate from the reaction mixture as highly crystalline solids which are pure as assessed by ^{1}H NMR spectroscopy. The cobalt complexes [(PATH)CoBr] (**4**) and [(PATH)CoNCS] (**5**) were prepared in a similar manner, except all manipulations had to be performed under strict exclusion of air. The availability of $Co(NCS)_2$ allowed for the synthesis of **5** by a more direct route than that used for **3**. These compounds can be prepared routinely as microcrystalline solids on a 0.5 g scale and can be stored in the solid state in a drybox for several weeks without noticeable decomposition.

Why Does PATH Give Monomeric Complexes? Some of the most successful ligands that have been used to date for modeling zinc metalloproteins similar to PDF have a tripodal[17] or macrocyclic[30] arrangement of donor groups. In

(30) Kimura, E.; Kikuta, E. *J. Biol. Inorg. Chem.* **2000**, *5*, 139−155.

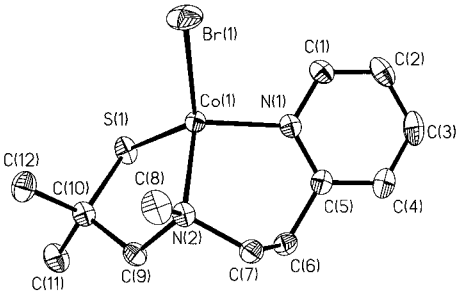

Figure 2. ORTEP diagram depicting the molecular structure of [(PATH)CoBr] (**4**) showing 50% probability ellipsoids and atom-labeling scheme. H atoms have been omitted for clarity.

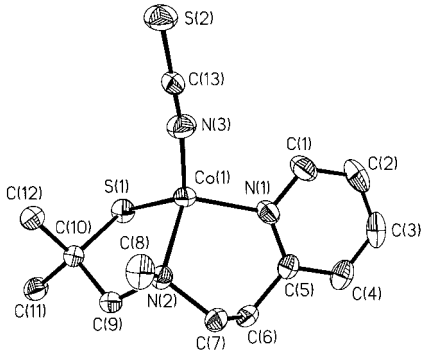

Figure 3. ORTEP diagram depicting the molecular structure of [(PATH)CoNCS] (**5**) showing 50% probability ellipsoids and atom-labeling scheme. H atoms have been omitted for clarity.

contrast, acyclic linear ligands like PATH are usually considered problematic for modeling such metalloproteins because of their inherent flexibility, which often leads to biologically irrelevant structural geometries.[17] For example, pyridine−amine−thiolate systems related to PATH that contain primary alkylthiolate arms invariably yield thiolate-bridged, polynuclear M^{II} complexes (M = Zn, Ni, Co, Fe, Mn).[31] We speculated that the inclusion of the *gem*-dimethyl groups in PATH would prevent M−S(R)−M bridges from forming. As shown in this work, the PATH ligand forms a series of discrete, mononuclear complexes of biological relevance. However, the *gem*-dimethyl substituents are only partly responsible for this success. A very similar N_2S-(thiolate) ligand recently reported by Vahrenkamp and co-workers, MBPAH (MBPAH = *N*-(2-mercaptoisobutyl)-(picolyl)amine), gives only polynuclear zinc species (e.g., $[(MBPA)Zn(OAc)]_2$) despite the incorporation of *gem*-dimethyl groups in the α-position to the sulfur atom.[16] The zinc ions are five-coordinate in this complex, and the thiolate donor of MBPA forms the bridges between zinc ions. It is intriguing to note that MBPA forms a five-membered chelate ring with the $N_{pyr}-C_{pyr}-CH_2-N_{amine}$ fragment, as opposed to the analogous six-membered ring of PATH. Thus it appears that the *gem*-dimethyl groups of PATH, in combination with the stability of the six-membered chelate ring that forms around a four-coordinate metal center, favor the formation of monomeric complexes.

Crystal Structures. The solid-state structures of [(PATH)-Co^{II}Br] and [(PATH)Co^{II}NCS] are shown in Figures 2 and 3. These complexes are isostructural with the zinc complexes **2** and **3**,[24] repectively. Pertinent bond length and angle information is given in Tables 2−4. The PATH ligand in the bromide complexes [(PATH)M^{II}Br] (M = Co, Zn) is coordinated in the expected tridentate fashion, and together with the Br^- ligand forms well-separated monomeric complexes whose geometry is best described as a distorted tetrahedron. The Zn−Br distance of 2.3277(5) Å for **2** matches well with other Zn−Br distances of four-coordinate Zn^{II} complexes with terminal bromide ligands.[32,33] Likewise, the Co^{II}−Br distance of 2.3810(5) Å for **4** falls within the range of known Co^{II}−Br bond lengths in tetrahedral Co^{II} complexes.[34,35] The thiocyanate complexes [(PATH)M^{II}NCS] (M = Co, Zn) exhibit the identical monomeric, pseudo-tetrahedral structures in which the NCS^- ligand has replaced the Br^- ligand in the open site. The thiocyanate ligands in **3** and **5** are coordinated through their nitrogen atoms at a distance of 1.961(3) Å for **3** and 1.9414(18) Å for **5** with a slightly bent M−N−C angle of 168° (173°) for **3** (**5**). These metrical parameters are similar to those for the tris-(pyrazolyl)borate complexes [(Tp^{tBu})ZnNCS] (Zn−N = 1.893(4) Å, Zn−N−C = 171.4(4)°)[36] and [(Tp^{tBu})CoNCS] (Co−N = 1.911(3) Å, Zn−N−C = 172.7°).[37]

The similarity in the effective ionic radii of cobalt(II) and zinc(II) is reflected in the mean $M-N_{PATH}$ distances in **2**, **3**, **4**, and **5** (2.08, 2.05, 2.06, and 2.05 Å, respectively), which correspond to that predicted from ionic radii (2.06 Å for Zn^{II} and 2.04 Å for Co^{II}).[38] The metal−sulfur bond distances for **2**−**5**, however, are significantly shorter than the distance expected from ionic radii, in keeping with an expected high degree of covalency for M−S bonds.[39,40] Other four-coordinate M^{II}−thiolate (M = Zn, Co) compounds with N_2S_2 donor sets, such as [Zn(S-2,4,6-$^iPr_3C_6H_2$)$_2$(bpy)] (mean Zn−S = 2.255(4) Å),[41] [Zn(MMP_2)] (HMMP = 2-mercaptomethylpyridine, mean Zn−S = 2.253(1) Å), [Co(S-2,4,6-$^iPr_3C_6H_2$)$_2$(py)$_2$] (mean Co−S = 2.263(3) Å),[42] and [Co(S-2,6-$^iPr_2C_6H_2$)$_2$(2,9-Me_2phen)] (mean Co−S = 2.244(2) Å),[43] exhibit similar M−S bond distances. Structural analysis of a series of five-coordinate, alkylthiolate−M^{II} complexes (M

(31) For a related series of such ligands, see the following. (a) Mikuriya, M.; Jian, X.; Ikemi, S.-i.; Kawahashi, T.; Tsutsumi, H. *Bull. Chem. Soc. Jpn.* **1998**, *71*, 2161−2168. (b) Mikuriya, M.; Kotera, T.; Adachi, F.; Handa, M.; Koikawa, M.; Okawa, H. *Bull. Chem. Soc. Jpn.* **1995**, *68*, 574−580. (c) Mikuriya, M.; Adachi, F.; Iwasawa, H.; Handa, M.; Koikawa, M.; Okawa, H. *Bull. Chem. Soc. Jpn.* **1994**, *67*, 3263−3270.
(32) Müller, B.; Vahrenkamp, H. *Eur. J. Inorg. Chem.* **1999**, 129−135.
(33) Yoon, K.; Parkin, G. *J. Am. Chem. Soc.* **1991**, *113*, 8414−8418.
(34) Kansikas, J.; Leskelä, M.; Kenessey, G.; Wadsten, T.; Liptay, G. *Acta Chem. Scand.* **1996**, *50*, 267−274.
(35) Caira, M. R.; Nassimbeni, L. R. *Acta Crystallogr.* **1974**, *B30*, 2332−2337.
(36) Looney, A.; Han, R.; Gorrell, I. B.; Cornebise, M.; Yoon, K.; Parkin, G.; Rheingold, A. L. *Organometallics* **1995**, *14*, 274−288.
(37) Trofimenko, S.; Calabrese, J. C.; Thompson, J. S. *Inorg. Chem.* **1987**, *26*, 1507−1514.
(38) Shannon, R. D. *Acta Crystallogr.* **1976**, *A32*, 751−767.
(39) Maelia, L. E.; Koch, S. A. *Inorg. Chem.* **1986**, *25*, 1896−1904.
(40) Shannon, R. D.; Vincent, H. In *Structure and Bonding in Crystals*; O'Keeffe, M., Navrotsky, A., Eds.; Springer-Verlag: New York, 1981; Vol. 2, Chapter 16.
(41) Corwin, D. T., Jr.; Koch, S. A. *Inorg. Chem.* **1988**, *27*, 493−496.
(42) Corwin, D. T., Jr.; Gruff, E. S.; Koch, S. A. *Chem. Commun.* **1987**, 966−967.
(43) Corwin, D. T., Jr.; Fikar, R.; Koch, S. A. *Inorg. Chem.* **1987**, *26*, 3080−3082.

Table 2. Selected Bond Distances (Å) and Angles (deg) for [(PATH)CoBr] (**4**)

Co(1)−N(1)	2.036(2)	Co(1)−N(2)	2.090(2)
Co(1)−S(1)	2.2327(7)	Co(1)−Br(1)	2.3810(5)
N(1)−C(5)	1.346(4)	N(1)−C(1)	1.352(4)
N(2)−C(8)	1.487(3)	N(2)−C(9)	1.499(3)
N(2)−C(7)	1.500(3)	S(1)−C(10)	1.849(3)
C(1)−C(2)	1.380(4)	C(2)−C(3)	1.387(5)
C(3)−C(4)	1.375(5)	C(4)−C(5)	1.401(4)
C(5)−C(6)	1.507(4)	C(6)−C(7)	1.530(4)
C(9)−C(10)	1.536(4)	C(10)−C(12)	1.528(4)
C(10)−C(11)	1.535(4)		
N(1)−Co(1)−N(2)	100.24(9)	N(1)−Co(1)−S(1)	119.72(7)
N(2)−Co(1)−S(1)	91.86(6)	N(1)−Co(1)−Br(1)	103.53(7)
N(2)−Co(1)−Br(1)	116.36(6)	S(1)−Co(1)−Br(1)	122.94(3)
C(5)−N(1)−C(1)	119.2(2)	C(5)−N(1)−Co(1)	121.24(19)
C(1)−N(1)−Co(1)	119.58(19)	C(8)−N(2)−C(9)	110.3(2)
C(8)−N(2)−C(7)	108.1(2)	C(9)−N(2)−C(7)	109.0(2)
C(8)−N(2)−Co(1)	110.98(18)	C(9)−N(2)−Co(1)	108.49(15)
C(7)−N(2)−Co(1)	109.93(16)	C(10)−S(1)−Co(1)	95.18(8)

Table 3. Selected Bond Distances (Å) and Angles (deg) for [(PATH)CoNCS] (**5**)

Co(1)−N(3)	1.9414(18)	Co(1)−N(1)	2.008(2)
Co(1)−N(2)	2.0839(18)	Co(1)−S(1)	2.2307(8)
N(1)−C(1)	1.352(3)	N(1)−C(5)	1.369(3)
N(2)−C(8)	1.493(3)	N(2)−C(7)	1.499(3)
N(2)−C(9)	1.504(3)	N(3)−C(13)	1.160(3)
S(1)−C(10)	1.854(2)	S(2)−C(13)	1.619(2)
C(1)−C(2)	1.367(4)	C(2)−C(3)	1.375(4)
C(3)−C(4)	1.381(4)	C(4)−C(5)	1.374(3)
C(5)−C(6)	1.504(3)	C(6)−C(7)	1.532(3)
C(9)−C(10)	1.543(3)	C(10)−C(12)	1.531(3)
C(10)−C(11)	1.539(3)		
N(3)−Co(1)−N(1)	107.85(8)	N(3)−Co(1)−N(2)	111.00(8)
N(1)−Co(1)−N(2)	100.81(8)	N(3)−Co(1)−S(1)	123.13(6)
N(1)−Co(1)−S(1)	117.11(5)	N(2)−Co(1)−S(1)	93.39(5)
C(1)−N(1)−C(5)	117.9(2)	C(1)−N(1)−Co(1)	120.76(17)
C(5)−N(1)−Co(1)	121.26(16)	C(8)−N(2)−C(7)	107.19(16)
C(8)−N(2)−C(9)	109.54(18)	C(7)−N(2)−C(9)	109.63(16)
C(8)−N(2)−Co(1)	113.15(14)	C(7)−N(2)−Co(1)	109.49(14)
C(9)−N(2)−Co(1)	106.87(12)	C(13)−N(3)−Co(1)	172.8(2)
C(10)−S(1)−Co(1)	91.79(7)	N(1)−C(1)−C(2)	123.8(2)
N(3)−C(13)−S(2)	179.7(2)		

= Zn, Co, Ni, Fe) by Kovacs has revealed the same covalent character for the metal−sulfur bonds.[44]

The PATH−Co^{II} bond distances for the bromide complex [(PATH)Co^{II}Br], Co^{II}−N(pyridine) = 2.036(2) Å, Co^{II}−N(amine) = 2.090(2) Å, and Co^{II}−S = 2.2327(7) Å, are slightly longer than the analogous bond lengths of 2.008(2), 2.0839(18), and 2.2307(8) Å for the cobalt thiocyanate complex [(PATH)CoNCS]. A similar trend is seen in the zinc complexes **2** and **3** (Table 4), and a comparison of the zinc tris(pyrazolylborate) complexes [(HB(^{t}Bupz)$_3$)ZnX] (X = Br, NCS) reveals the same metrical trend, i.e., Zn−$N(pz)_{av}$ = 2.059 Å for X = Br,[33] and Zn−$N(pz)_{av}$ = 2.033 Å for X = NCS.[36] This effect is unlikely due to steric constraints since the steric crowding at the metal center is quite different for the PATH ligand as compared to the HB(^{t}Bupz)$_3$ ligand, yet the same trend is observed. These data suggest that the bromide ion is a slightly stronger donor than the thiocyanate ligand, in contrast to what one would predict from the pK_a values of their conjugate acids (for HBr,[45] pK_a ∼ −9; for HSCN,[46,47] pK_a = −2.0−0.9).

Comparison of Models with Zn−PDF and Co−PDF Structures. The structures of the zinc model complexes **2** and **3** are compared in Table 4 with the recently reported 1.9 Å resolution crystal structure of Zn−PDF, in which the fourth ligand is a water molecule.[8c] In this structure there are three independent zinc centers, which give average zinc−ligand distances of Zn−Cys90 = 2.1 Å, Zn−His132 = 2.1 Å, and Zn−His136 = 2.1 Å. These are reproduced well by the Zn−N and Zn−S distances in complexes **2** and **3**. In addition, the angles defining the distorted tetrahedral zinc atoms of **2** and **3** have a striking similarity with the angles found for the zinc center in PDF (Table 4), especially the two obtuse angles containing the sulfur ligand (e.g., **3**, S−Zn−X = 121° (123°), X = $N_{pyridine}$ (NCS); Zn−PDF, S−Zn−X = 117° (134°), X = N_{His132} (O_{water})). It is likely that the large size of the sulfur atom causes the same distortions from tetrahedral geometry in both models and protein, resulting in two angles being significantly wider than the ideal 109.5°. The sole Co^{II}−PDF structure reported thus far, which contains a bound phosphate group as the fourth ligand to cobalt,[8a] exhibits similar obtuse angles in the metal coordination sphere (N_{His132}−Co^{II}−S_{Cys90} = 117°, $O_{inhibitor}$−Co^{II}−S_{Cys90} = 132°). Interestingly, the Co^{II}−N distances in this structure are in the same range as those in our model complexes (Co^{II}−N_{His132} = 2.086 Å, Co^{II}−N_{His136} = 2.096 Å), but the Co^{II}−S_{Cys90} distance of 2.379 Å is significantly longer than Co^{II}−S = 2.2327(7) Å for **4** and Co^{II}−S = 2.2307(8) Å for **5**.

Stereochemistry. Formation of complexes **2**−**5** generates two chiral centers, one at the metal atom and the other at the tertiary N atom. In one pair of enantiomers the N−CH_3 group and the terminal zinc ligand (Br or NCS) are on the same side of the fused 5,6-membered chelate rings (cis diastereomer), while in the other pair they are located on opposite sides (trans diastereomer). Compounds **2**−**5** exist as a racemic mixture of the cis diastereomer.

Solution-State Structure and Energetic Preference for the Cis Diastereomer. The ^{1}H NMR data for **2** and **3** confirm the presence of one diastereomer and provide good evidence that the solution state structure is identical to that observed in the crystal. For example, there are only two resonances observed for each of the diastereotopic *gem*-dimethyl groups, and complex splitting patterns are seen for the −CH_2CH_2− fragment. Although these NMR data cannot prove the existence of the cis isomer in solution, it seems unlikely that the trans isomer is stable in solution while the cis isomer is exclusively observed in the solid state. Moreover, we have evaluated the relative energies of the cis and trans isomers for [(PATH)Co^{II}Br] by molecular mechanics calculations (MM2 force field) using the Chem3D Pro suite of programs.[48] Interestingly, the cis diastereomer

(44) Shoner, S. C.; Nienstedt, A. M.; Ellison, J. J.; Kung, I. Y.; Barnhart, D.; Kovacs, J. A. *Inorg. Chem.* **1998**, *37*, 5721−5726.

(45) Gordon, A. J.; Ford, R. A. *The Chemist's Companion*; John Wiley & Sons: New York, 1972.

(46) Boughton, J. H.; Keller, R. N. *J. Inorg. Nucl. Chem.* **1966**, *28*, 2851−2859.

(47) Morgan, T. D. B.; Stedman, G.; Whincup, P. A. E. *J. Chem. Soc.* **1965**, 4813−4822.

(48) *Chem3D Pro 3.2* for Macintosh, Cambridge Scientific Computing, Inc., Cambridge, MA.

Table 4. Comparison of Selected Bond Distances (Å) and Angles (deg) for Complexes **2**−**5**, Zn^{II}−PDF, and Co^{II}−PDF

	2[a,b] (M = Zn)	**4**[b] (M = Co)	**3**[a,c] (M = Zn)	**5**[c] (M = Co)	Zn^{II}−PDF[d,e]	Co^{II}−PDF[f,g]
M−$S_{thiolate}$	2.2548(7)	2.2327(7)	2.2413(8)	2.2307(8)	2.1	2.4
M−N(1)	2.058(2)	2.036(2)	2.022(2)	2.008(2)	2.1	2.1
M−N(2)	2.110(2)	2.090(2)	2.086(3)	2.0839(18)	2.1	2.1
M−X	2.3777(5)	2.3810(5)	1.961(3)	1.9414(18)	1.9	2.2
$S_{thiolate}$−M−N(1)	120.92(7)	119.72(7)	120.57(7)	117.11(5)	117	117
$S_{thiolate}$−M−N(2)	92.88(6)	91.86(6)	94.73(7)	93.39(5)	105	96
$S_{thiolate}$−M−X	123.30(3)	122.94(3)	122.88(8)	123.13(6)	133	132
N(1)−M−X	102.15(17)	103.53(7)	104.29(11)	107.85(8)	96	100
N(2)−M−X	116.04(7)	116.36(6)	110.79(11)	111.00(8)	93	104
N(1)−M−N(2)	99.29(9)	100.24(9)	100.51(10)	100.81(8)	107	102
M−N(3)−C_{NCS}			168.3(3)	172.8(2)		

[a] Chang, S.; Karambelkar, V. V.; diTargiani, R. C.; Goldberg, D. P. *Inorg. Chem.* **2001**, *40*, 194−195. [b] X = Br. [c] X = NCS. [d] Becker, A.; Schlichting, I.; Kabsch, W.; Groche, D.; Schultz, S.; Wagner, A. F. V. *Nat. Struct. Biol.* **1998**, *5*, 1053−1058. [e] X = H_2O, N(1) = His132, N(2) = His136. [f] Hao, B.; Gong, W.; Rajagopalan, P. T. R.; Zhou, Y.; Pei, D.; Chan, M. K. *Biochemistry* **1999**, *38*, 4712−4719. [g] X = (*S*)-2-*O*-(H-phosphonoxy)-L-leucyl-*p*-nitroanilide, N(1) = His132, N(2) = His136.

(minimized steric energy = 25.4 kcal/mol) is ca. 13 kcal/mol lower in energy than the trans isomer (minimized steric energy = 38.2 kcal/mol),[49] and the $-CH_2CH_2-$ unit in the cis diastereomer adopts a significantly more staggered orientation than that of the trans isomer in the energy-minimized structures. Although these calculations are low level, they are in good agreement with the experimental observation that the cis is the more stable isomer. We conclude that the cis diastereomer is formed preferentially over the trans because of the relatively low energy conformation obtained in the $-CH_2CH_2-$ fragment for the cis diastereomer.

Formation of [(PATH)Zn(OH)]. Only a handful of monomeric zinc hydroxide compounds have been successfully isolated, and the first sulfur-containing example, [Tm^{Ph}]-ZnOH (Tm^{Ph} = tris(2-mercapto-1-phenylimidazolyl)hydroborate), was unknown until very recently.[50] Although we have not yet succeeded in isolating [(PATH)Zn(OH)] as a pure crystalline solid, the titration of **2** as monitored by ^{1}H NMR spectroscopy indicates that [(PATH)Zn(OH)] is formed in situ by the displacement of Br^- with OH^-. Addition of successive amounts of NaOH in D_2O to a solution of **2** in CD_3OD results in the series of spectra shown in Figure 4. As seen in the figure, there is a small but definite shift upfield for the resonance of the H_α proton, which is close to the labile Br^- ligand. The H_α peak for pure [(PATH)ZnBr] at 8.72 ppm shifts upfield with the addition of increasing amounts of hydroxide anion until 1.4 equiv has been added, resulting in a final shift of $\delta(H_\alpha)$ = 8.62 ppm. As seen in Figure 4, the peaks from the other pyridine protons do not shift during the titration. Some minor shifts are observed in the signals for some of the other ligand resonances, but the overall features of the spectra do not change throughout the titration.

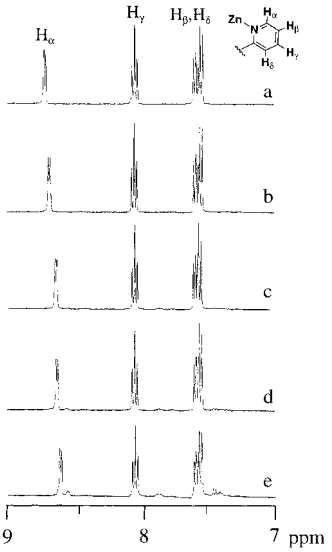

Figure 4. ^{1}H NMR spectra of [(PATH)ZnBr] in CD_3OD (13.6×10^{-3} M) after the addition of varying amounts of NaOH in D_2O at 24 °C: (a) 0 equiv of NaOH; (b) 0.4 equiv of NaOH; (c) 0.8 equiv of NaOH; (d) 1.0 equiv of NaOH; (e) 1.4 equiv of NaOH. As the amount of OH^- is increased, the H_α resonance shifts upfield, consistent with the substitution of OH^- for Br^- anion and formation of [(PATH)Zn(OH)].

These data suggest that the bromide ligand in **2** is quantitatively displaced with OH^- anion, and the monomeric, four-coordinate structure remains intact to give [(PATH)-ZnOH]. It has been shown previously that the chemical shift of the H_α resonance is sensitive to the nature of the fourth ligand in the labile position (e.g., for [(PATH)ZnNCS] $\delta(H_\alpha)$ = 8.54 ppm in CD_3CN versus 8.70 ppm for **2**) and is a useful marker for following ligand substitutions at the labile site.[24] If binding of hydroxide were giving the 5-coordinate complex [(PATH)Zn(OH)(Br)], more dramatic changes in the ^{1}H NMR spectrum would be expected. Addition of more than 1 equiv of OH^- causes the appearance of new peaks at δ 8.55, 7.88, and 7.42 ppm (see Figure 4e), suggesting the formation of another species. The [(PATH)Zn(OH)] species that forms after addition of 1 equiv OH^- appears stable, and

(49) The bulk of the MM2 parameters included in the *Chem3D Pro* software are best described in the following: Burkert, U.; Allinger, N. L. *Molecular Mechanics*; ACS Monograph 177; American Chemical Society: Washington, DC, 1982. Additional parameters were provided by Dr. Jay Ponder, Washington University, author of the TINKER program, and CambridgeSoft Corporation. Parameters for transition metals such as Co(II) are not well-supported by MM2, and minimizations were preformed in which the optimal N−Co(II) and S−Co(II) bond distances were taken from the X-ray structure of **4**. In addition, after an initial minimization, the torsion angle defined by C(2)−C(1)−N(1)−Co(1) was set to 180°, and these atoms were then fixed in position prior to a final minimization. The final refined structure for the cis form of **4** was in good agreement with the X-ray structure. In particular, the torsion angles around the $-CH_2CH_2-$ fragment were close to the experimentally determined values.

(50) Bridgewater, B. M.; Parkin, G. *Inorg. Chem. Commun.* **2001**, *4*, 126−129.

Table 5. UV−Vis Data for [(PATH)CoBr], [(PATH)CoNCS], Wild-Type and Mutant Co^{II}−PDF, and Co^{II}-Substituted Blue Copper Proteins Stellacyanin, Mavicyanin, and Pseudoazurin, λ_{max}, nm (ϵ, M^{-1} cm^{-1})

compound	LMCT	d−d transitions	ref
[(PATH)CoBr]	315 (3032), 388 (1294), 414 (1465)	538 (270), 643 (sh, 460), 672 (522)	*c*
[(PATH)CoNCS]	326 (3861), 375 (1332), 443 (877)	517 (290), 622 (394), 669 (489)	*c*
Co^{II}−PDF	325 (1100)	565 (580), 640 (∼170), 660 (∼170)	13
Co−PDF (E133A)[a]		565 (>600), 605 (>600), 650 (>600)	13
stellacyanin	310 (sh), 365 (∼2000),	540 (∼300), 625 (∼450), 640 (∼450)	54, 55, 70
mavicyanin[b]	336 (1300)	539 (260), 620 (330), 655 (370)	64
pseudoazurin	335 (∼1900), 390 (sh), 440 (sh)	505 (∼250), 640 (sh), 673 (∼280)	63

[a] The fourth ligand is Cl^-. [b] pH = 11.0 [c] This work.

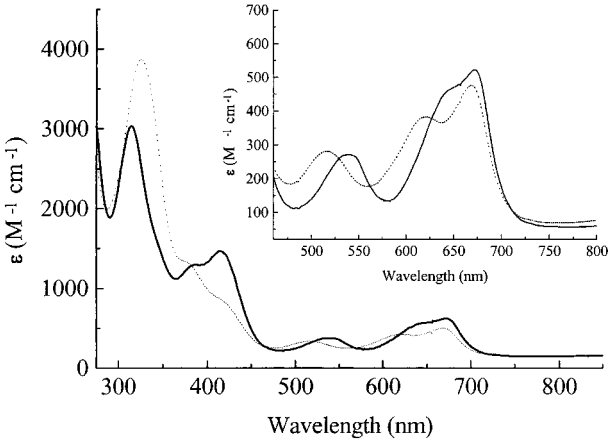

Figure 5. UV−vis spectra of [(PATH)CoBr] (**4**) (1.5 mM) (solid line) and [(PATH)CoNCS] (**5**) (0.79 mM) (dashed line) in CH_3CN. Inset: Expanded region showing the d−d transitions for **4** (0.55 mM) (solid line) and **5** (0.50 mM) (dashed line).

attempts to isolate it in pure form are underway along with studies to examine its hydrolytic activity.[51]

UV−Vis Studies. (a) Assignment of Bands. The electronic absorption spectra for compounds **4** and **5** in CH_3CN are shown in Figure 5 and can be compared with data from Co^{II}−PDF and the related His_2Cys centers in cobalt-substituted blue copper proteins (Table 5). The cobalt complexes exhibit intense bands at 315 nm (**4**) and 326 nm (**5**), which are in the range for S → Co^{II} charge-transfer transitions.[42,52−55] In the case of the bromide complex, two additional peaks are observed at 388 and 414 nm, which can also be ascribed to S → Co^{II} LMCT bands.[42,52−55] The thiocyanate complex exhibits similar low-energy S → Co^{II} LMCT peaks at 375 and 443 nm. Compounds **4** and **5** each exhibit three bands between 500 and 700 nm which are characteristic of the $^4A_2 \rightarrow {}^4T_1(P)$ d−d transitions observed for a high-spin Co^{II} ion in a tetrahedral environment.[52,56] Extinction coefficients for Co^{II} d−d transitions have been correlated previously with the coordination number such that a four-coordinate ion has d−d bands with $\epsilon \sim 300$ M^{-1} cm^{-1} or greater, a five-coordinate ion has 50 M^{-1} $cm^{-1} < \epsilon <$ 300 M^{-1} cm^{-1}, and a six-coordinate Co^{II} exhibits peaks with $\epsilon < 50$ M^{-1} cm^{-1}.[52,54,57] The extinction coefficients for **4** and **5** (Table 5) are in line with that expected for a tetrahedral cobalt(II) ion.

(b) UV−Vis Spectra for 4 and 5 in Donating versus Nondonating Solvents. Dissolution in donating (CH_3CN, MeOH) or nondonating (CH_2Cl_2) solvents has little effect on the color or electronic spectra of **4** or **5**. In comparison, complexes such as $[Co^{II}(HB(3\text{-}i\text{-}Prpz)_3)X]$[58] (X = NCO, NCS) or $[Co^{II}(HB(3\text{-}Phpz)_3)X]$[37,59] (X = NCS) exhibit dramatic spectral changes upon shifting from a nondonating solvent to a donating solvent such as THF. Although the former tris(pyrazolyl)borate ligands provide considerable steric encumberance around the metal center, donating solvents still bind to give a five-coordinate Co^{II} ion. Remarkably, we do not see any evidence of solvent coordination in our complexes even though our PATH ligand provides little steric protection against solvent accessibility.

(c) Comparison of UV−Vis Spectra of PATH−Co^{II} Model Complexes with Co^{II}-Substituted Metalloproteins. The UV−vis spectra for Co^{II}−PDF have recently been reported by Pei et al.[13] At neutral pH, the wild-type cobalt-(II)-substituted protein has a bound water molecule as the fourth ligand. The UV−vis spectrum of this form of the protein exhibits a S → Co^{II} CT band as expected, but the d−d bands at lower energy (640 and 660 nm) are significantly weaker in intensity than the d−d band at 565 nm, which contrasts the spectra observed for **4** and **5** and the other proteins in Table 5. The cobalt-substituted E133A PDF mutant, with a $[His_2CysCo^{II}(Cl)]$ metal center, also exhibits an overall shape rather different from **4** or **5**. However, the spectrum of [(PATH)Co(OH)], formed in situ from **4**, strongly resembles the high-pH spectrum of the E133A Co^{II}−PDF, assigned to a Co−OH species (vide infra).[13]

(51) Evidence against the formation of [(PATH)Zn(OMe)] comes from examining the reaction between NaOMe and [(PATH)ZnBr]. Addition of 1 equiv of dry NaOMe to [(PATH)ZnBr] in CD_3OD (air-free) results in a very small upfield shift (∼0.02 ppm) for H_α, compared to the 0.1 ppm shift seen for 1 equiv of OH^-. Moreover, the few well-characterized monomeric Zn−OH complexes have been prepared from the addition of OH^- in MeOH, and formation of Zn−OH has been shown to be thermodynamically favored over Zn−OMe: (a) Bergquist, C.; Parkin, G. *Inorg. Chem.* **1999**, *38*, 422. (b) Alsfasser, R.; Trofimenko, S.; Looney, A.; Parkin, G.; Vahrenkamp, H. *Inorg. Chem.* **1991**, *30*, 4098−4100.

(52) Lever, A. B. P. *Inorganic Electronic Spectroscopy*; Elsevier: Amsterdam, 1984.
(53) Lane, R. W.; Ibers, J. A.; Frankel, R. B.; Papaefthymiou, G. C.; Holm, R. H. *J. Am. Chem. Soc.* **1977**, *99*, 84−98.
(54) McMillin, D. R.; Holwerda, R. A.; Gray, H. B. *Proc. Natl. Acad. Sci. U.S.A.* **1974**, *71*, 1339−1341.
(55) McMillin, D. R.; Rosenberg, R. C.; Gray, H. B. *Proc. Natl. Acad. Sci. U.S.A.* **1974**, *71*, 4760−4762.
(56) Banci, L.; Bencini, A.; Benelli, C.; Gatteschi, D.; Zanchini, C. *Struct. Bonding (Berlin)* **1982**, *52*, 37−86.
(57) Bertini, I.; Luchinat, C. In *The Reaction Pathways of Zinc Enzymes and Related Biological Catalysts*; Bertini, I., Gray, H. B., Lippard, S., Valentine, J., Eds.; University Science Books: Mill Valley, 1994; pp 37−106.
(58) Trofimenko, S.; Calabrese, J. C.; Domaille, P. J.; Thompson, J. S. *Inorg. Chem.* **1989**, *28*, 1091−1101.
(59) Kremer-Aach, A.; Klâui, W.; Bell, R.; Strerath, A.; Wunderlich, H.; Mootz, D. *Inorg. Chem.* **1997**, *36*, 1552−1563.

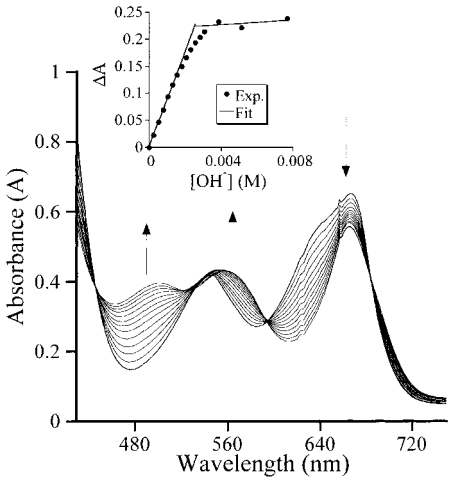

Figure 6. UV−vis spectrum of [(PATH)CoBr] (**4**) in CH_3OH (2.54×10^{-3} M) after the addition of varying amounts of NaOH. Inset: Plot of ΔA vs [OH^-] for the absorbance at 480 nm ($\Delta A = A - A_0$; $A_0 = 0$ equiv of OH^-). The lines were obtained from a least-squares fit of the linear portions of the curve.

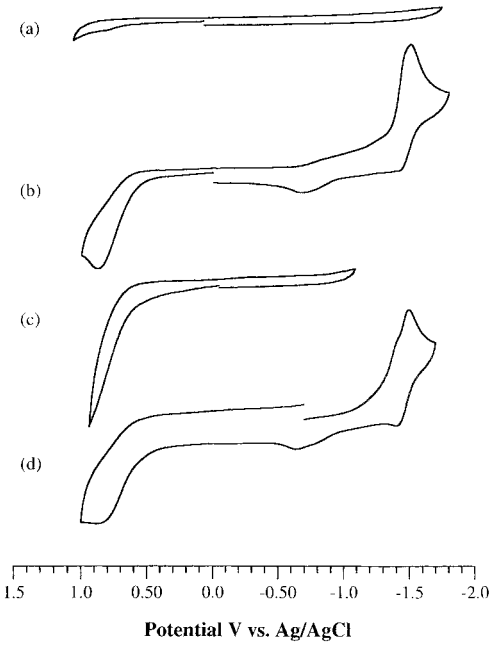

Figure 7. Cyclic voltammograms in CH_3CN with 0.2 M Bu_4NPF_6 added as electrolyte of (a) [(PATH)ZnBr] (**2**) (500 mV/s), (b) [(PATH)CoBr] (**4**) (200 mV/s), (c) [(PATH)CoBr] (500 mV/s; negative limit = −1000 mV, positive limit = +950 mV), and (d) [(PATH)CoNCS] (500 mV/s).

The UV−vis spectra of Co^{II}-substituted blue copper proteins warrant brief discussion here since the defining structural motif for these proteins is the same $(His)_2(Cys)$-$M^{II}L$ center found in PDF, and a large amount of effort has been expended on their spectroscopic characterization. Model complexes **4** and **5** exhibit UV−vis spectra that bear a striking similarity with those of the Co^{II}-substituted blue copper proteins stellacyanin, pseudoazurin, and mavicyanin, which have a more tetrahedral, as opposed to trigonal planar, metal center. The recent X-ray structure[60] of stellacyanin reveals a distorted tetrahedral copper center, [$Cu^{II}(His_2Cys)$-(OC-Gln)], similar in geometry to the rhombic (T1) copper site found in pseudoazurin,[61] and in contrast to the more common trigonal planar arrangement of the His_2Cys ligands found in the axial T2 center of proteins such as plastocyanin.[61] Specifically, the high-energy S → Co^{II} LMCT band for **4** and **5** is similar to the S(cys) → Co^{II} charge-transfer band (310 nm) found for *Rhus vernicifera* stellacyanin, which is significantly blue-shifted from the peak at 333 nm seen in *Phaseolus vulgaris* plastocyanin.[54,55,62] In addition, the position, intensities, and overall shape of the d−d bands for **4** and **5** are close to those found for stellacyanin,[54,55,62] pseudoazurin,[63] and mavicyanin.[64]

Formation of [(PATH)Co(OH)]. As in the case of Zn^{II}, a monomeric Co^{II}−hydroxide or −water complex is particularly important in the quest to build *hydrolytically active* N_2S model complexes. Evidence for the formation of the hydroxide complex [(PATH)Co(OH)] comes from the UV−vis titration shown in Figure 6. A solution of **4** in MeOH was titrated with a concentrated stock solution of NaOH in H_2O (0.1−3.0 equiv of OH^-). The reaction equilibrated rapidly as noted by an immediate change in the absorption spectrum within the first minute of mixing followed by no change in the spectrum. As seen in the figure, isosbestic points are observed at $\lambda = 447$, 597, and 685 nm, suggesting that only two species are present throughout the titration. A plot of ΔA versus [OH^-] is shown in the inset of Figure 6 and is consistent with tight 1:1 binding of hydroxide to the cobalt complex. The stoichiometry is supported by the fact that best-fit lines drawn through the initial linear and final plateau regions of the curve intersect near 1 equiv of OH^- (the mole-ratio method).[65] The final spectrum of the OH^- complex exhibits peaks at $\lambda_{max} = 490$, 560, and 665 nm and is quite similar to the spectrum of Co−OH peptide deformylase (pH > 10; $\lambda_{max} = 510$, 550, and 675 nm).[13] Taken all together these data are most simply explained by the formation of [(PATH)Co(OH)].[66] The high binding affinity of OH^- versus Br^- corresponds to similar observations made for PDF; competition experiments between OH^- and a halide ion (Cl^-) reveal that OH^- ion binds ~10^5 times more tightly than Cl^- ion to the metal center in E133A Co^{II}PDF.[13]

Electrochemistry. The cyclic voltammograms for [(PATH)-ZnBr] (**2**), [(PATH)CoBr] (**4**), and [(PATH)CoNCS] (**5**) are shown in Figure 7. As can be seen from the figure, the cobalt complexes exhibit similar electrochemical behavior (Figure 7b and Figure 7d), indicating that the identity of the fourth

(60) Hart, J. P.; Nersissian, A. M.; Herrmann, R. G.; Nalbandyan, R. M.; Valentine, J. S.; Eisenberg, D. *Protein Sci.* **1996**, *5*, 2175−2183.
(61) Andrew, C. R.; Yeom, H.; Valentine, J. S.; Karlsson, B. G.; Bonander, N.; Pouderoyen, G. v.; Canters, G. W.; Loehr, T. M.; Sanders-Loehr, J. *J. Am. Chem. Soc.* **1994**, *116*, 11489−11498 and references therein.
(62) Strong, C.; Harrison, S.; Zeger, W. *Inorg. Chem.* **1994**, *33*, 606−608.
(63) Suzuki, S.; Sakurai, T.; Shidara, S.; Iwasaki, H. *Inorg. Chem.* **1989**, *28*, 802.
(64) Maritano, S.; Marchesini, A.; Suzuki, S. *J. Biol. Inorg. Chem.* **1997**, *2*, 177−181.
(65) Skoog, D. A.; West, D. M. *Fundamentals of Analytical Chemistry*, 3rd ed.; Holt, Rinehart, and Winston: New York, 1976.
(66) The reaction between NaOMe and [(PATH)CoBr] in dry MeOH resulted in the same change in the UV−vis spectrum, but this is not surprising since [(PATH)Co(OMe)] and [(PATH)Co(OH)] should exhibit quite similar absorption spectra given their similarities in donor sets and expected geometry. See ref 51.

ligand, Br^- or NCS^-, does not have a significant effect on the redox properties of the metal. The [(PATH)ZnBr] complex does not show any electrochemical activity in this region (Figure 7a), indicating that PATH is not redox-active in these complexes. A quasi-reversible reduction peak is observed for the cobalt bromide complex at −1.51 and −1.49 V for the cobalt thiocyanate complex, which we assign for both compounds as a Co^{II}/Co^{I} process. Some of the Co^{I} species undergoes a fast chemical transformation to an unidentified product (vide infra).

For comparison, the pseudotetrahedral N_4Co^{II} complexes [Co(^{Bz}DATI)$_2$] and [Co(^{iPr}DATI)$_2$] (DATI = dansyl-aminotroponiminate) exhibit Co^{II}/Co^{I} couples at potentials very close to those seen for the PATH complexes.[67] In the DATI complexes the cobalt ion is bound by two bidentate nitrogen chelates of −1 charge, and quasi-reversible waves for the Co^{II}/Co^{I} process are observed at −2.09 and −1.98 V versus Cp_2Fe^+/Cp_2Fe, respectively. The recently described S_3Co^{II}-Cl complex [PhTt^{t-Bu}]Co^{II}Cl (PhTt^{t-Bu} = phenyltris((*tert*-butylthio)methyl)borate) exhibits an irreversible reduction at −1.51 V (vs Cp_2Fe^+/Cp_2Fe in CH_2Cl_2) that can be ascribed to a Co^{II}/Co^{I} process.[68] In [PhTt^{t-Bu}]Co^{II}Cl the cobalt ion is bound by three thioether donors that insulate it from the negative charge on the boron atom. In contrast, the PATH or DATI complexes each have two anionic ligands bound directly to the metal center, and these structural differences may account for the fact that the Co^{II}/Co^{I} reduction for [PhTt^{t-Bu}]Co^{II}Cl occurs ∼500 mV more positive than in the PATH or DATI complexes.[69]

There are two irreversible oxidation peaks seen at ∼−0.65 V and +0.90 V for both **4** and **5**. The former peak is not observed in cycles in which the negative potential limit is more positive than ∼−1.2 V (Figure 7c), i.e., when there is no reduction of Co^{II} to Co^{I}, leading us to assign this peak to an unidentified species formed immediately after reduction of the starting complex. The anodic peak at +0.90 V is likely the Co^{III}/Co^{II} couple, which is irreversible regardless of solvent (DMF, CH_3CN, CH_2Cl_2) or scan rate (25−2000 mV/s). Slow electrode-to-complex electron-transfer kinetics is often observed for Co^{III}/Co^{II} couples and is likely responsible for the irreversible nature of this peak.

(67) Franz, K. J.; Singh, N.; Spingler, B.; Lippard, S. J. *Inorg. Chem.* **2000**, *39*, 4081−4092.
(68) Schebler, P. J.; Riordan, C. G.; Guzei, I. A.; Rheingold, A. L. *Inorg. Chem.* **1998**, *37*, 4754−4755.
(69) Another Co^{II} complex which has not been crystallographically characterized but is presumed to have an NNSO donor set exhibits an irreversible reduction at −0.96 V (vs SCE in DMF, ∼−1.5 V vs Fc^+/Fc). See the following: Adhikary, B.; Nanda, K. K.; Das, R.; Mandal, S. K.; Nag, K. *Polyhedron* **1992**, *11*, 347−353.
(70) Solomon, E. I.; Rawlings, J.; McMillin, D. R.; Stephens, P. J.; Gray, H. B. *J. Am. Chem. Soc.* **1976**, *98*, 8046−8048.

Concluding Remarks

The new N_2S(thiolate) ligand PATH yields a series of monomeric Zn^{II} and Co^{II} model complexes that bear good resemblance to the His_2Cys-M^{II} active site found in PDF. Moreover, the synthesis of PATH−H involves a facile one-step procedure on the multigram scale, in contrast to the typically more difficult syntheses of the "tetrahedral enforcer" ligands of the tripodal or macrocyclic type. Thus, the notion that a tripodal or otherwise constrained ligand system is required in order to give monomeric, tetrahedral model complexes has been disproven. The prevalence of monomeric compounds in this study is likely due to a combination of steric encumbrance of the thiolate donor and the stable conformation adopted by the PATH ligand.

The cobalt compounds [(PATH)CoBr] and [(PATH)-CoNCS] are the first examples of structurally well-defined Co^{II} complexes with an N_2SL (L ≠ N,S) donor set. They are isostructural with their Zn^{II} counterparts, and these data add credence to the accepted idea that Co^{II} is an appropriate spectroscopic probe for biological Zn^{II} sites. It is interesting to compare our results with those of Klaui and co-workers, who recently described a series of tris(pyrazolyl)borate zinc(II) and cobalt(II) complexes that display significant structural differences.[59] The cobalt complexes have been characterized by UV−vis spectroscopy and cyclic voltammetric measurements. The UV−vis spectra of **4** and **5** show that they are monomeric, 4-coordinate species in solution, and these complexes provide spectroscopic benchmarks for similar 4-coordinate, N,S(thiolate) Co^{II} centers in metalloproteins.

In our efforts to move toward hydrolytically functional model complexes, 1:1 metal:hydroxide species of PATH−Zn^{II} and PATH−Co^{II} were formed in situ by substitution of a labile bromide ligand with hydroxide anion. In the case of Co^{II}, the hydroxide complex exhibits a UV−vis spectrum that is quite similar to Co^{II}-OH PDF. Efforts to isolate and characterize the hydroxide complexes as crystalline solids, as well as the preparation of Ni^{II} and Fe^{II} complexes of PATH will be described in due course.

Acknowledgment. This work was supported by NIH Grant GM 62309 (to D.P.G.). We are grateful to Dr. J. Kachinski for collection of the FAB mass spectra. We thank Prof. G. Meyer for the use of his electrochemistry apparatus.

Supporting Information Available: X-ray crystallographic information for [(PATH)CoBr] (**4**) and [(PATH)CoNCS] (**5**), including atomic positional and thermal parameters, bond distances and angles, and calculated hydrogen atom positional parameters. This material is available free of charge via the Internet at http://pubs.acs.org.

IC010321R